Green Chemistry

PAPER

View Article Online
View Journal | View Issue

Cite this: *Green Chem.*, 2014, **16**, 3942

Hemicellulose-derived chemicals: one-step production of furfuryl alcohol from xylose†

Rafael F. Perez and Marco A. Fraga*

Received 6th March 2014,
Accepted 13th June 2014

DOI: 10.1039/c4gc00398e

www.rsc.org/greenchem

One-pot production of furfuryl alcohol *via* xylose dehydration followed by furfural hydrogenation was investigated over a dual catalyst system composed of Pt/SiO_2 and sulfated ZrO_2 as metal and acid catalysts, respectively. All samples were characterized by XRD, XRF, N_2 physisorption, TG-MS and FTIR regarding their most fundamental properties for the studied process. A systematic study is reported on the effects of the reaction temperature, the composition of the binary solvent and the molar ratio between acid and metal sites in the catalyst system. The results revealed the feasibility of the one-step process for furfuryl alcohol synthesis and showed that the occurrence of both acid and metal sites is compulsory in order to promote the dehydration of xylose to furfural and its further hydrogenation to furfuryl alcohol. Selectivity towards furfuryl alcohol was found to be strongly dependent on the solvent, which can inhibit its polymerization to some extent.

Introduction

The production of chemical compounds has been pursuing a different course with the adoption of the principles of sustainable development. Aware of the need to reduce environmental impacts, chemical industries have been making efforts to reduce, or even replace, the use of fossil resources moving to the conversion of renewable raw materials.

Lignocellulosic biomass stands out as an ideal renewable feedstock for this purpose since it is a low-cost abundant supply. Its use should not compete with food production and the large availability may guarantee the bulk production of bio-based-chemicals and fuels. Lignocellulose is typically composed of approximately 75% of carbohydrates (cellulose and hemicellulose) and around 20% of lignin. These biopolymers can be converted into platform molecules for the production of high-value-added chemicals.[1–3] While C6 sugars released from cellulose have been mostly aimed for second-generation ethanol production, hemicellulose-derived monosaccharides appear as very important feedstock to synthesize green chemicals.

As a matter of fact, much attention has been devoted to hemicellulose, which is a branched heteropolysaccharide made up of several C6 and C5 monosaccharide units, particularly xylose and arabinose. These pentoses may be converted into a wide range of compounds; xylose is, industrially, mostly used to produce furfural (2-furaldehyde) through dehydration using mineral acids as homogeneous catalysts.[4] This process generates highly polluting effluents that should be treated on site, requires a lot of energy and only achieves low yields (less than 50%).[5] Over the last few years, many studies have searched for new sustainable ways of producing furfural using heterogeneous acid catalysts, tuning the temperature, pressure and solvent and exploiting different extracting techniques to increase the aldehyde yield.[1,2,6–18]

About 60% of the world production of furfural is used for obtaining furfuryl alcohol,[19] which is an important monomer in the polymer industry to fabricate poly(furfuryl alcohol), a chemical resistant resin. Furfural is also used to produce synthetic fibers, epoxy and phenolic resins and is a precursor for the production of 2-methylfuran, 2-methyltetrahydrofuran and levulinic acid.[1]

The reduction of furfural to its alcohol derivatives is industrially carried out by catalytic hydrogenation in the liquid or vapor phase using a heterogeneous chromium-based catalyst.[1] Due to its carcinogenic potential, much effort has been made to replace these catalysts with non-toxic materials. RANEY®-type catalysts and noble metals supported on oxides are among the major systems investigated.[1,2,20–22]

Even though promising results have been reported to overcome the drawbacks of each of these reactions separately – dehydration of xylose and furfural hydrogenation – at present, furfuryl alcohol may only be produced by a two-step process based on catalysts with distinct features and operating at different conditions. As far as we know, there is no information, in the literature, on the production of furfuryl alcohol

Instituto Nacional de Tecnologia/MCTI, Divisão de Catálise e Processos Químicos, Av. Venezuela, 82/518, Centro, 20081-312 Rio de Janeiro, Brazil.
E-mail: marco.fraga@int.gov.br

†Electronic supplementary information (ESI) available. See DOI: 10.1039/c4gc00398e

directly from xylose in a single step. The development of a straightforward process by making use of selective catalytic systems would lead to a lower demand for energy by reducing the number of reaction steps and the amount of wastage. The employment of heterogeneous systems can also allow separation, recovery and reuse of the catalyst.

This paper reports an innovative process to obtain furfuryl alcohol from xylose over a dual heterogeneous catalyst system that allows the reaction to occur in a single step and with high selectivity. In this contribution, the effects of the reaction temperature, the ratio of metal and acid sites and the composition of the solvent on furfuryl alcohol selectivity are investigated.

Experimental

A commercially available sulfated zirconia (ZrO_2–SO_4) from Mel Chemicals (ref. XZO 1249) and a Pt/SiO_2 catalyst prepared in the laboratory were used as heterogeneous catalysts.

Prior to use, the acid catalyst was thermally treated in an oven at 600 °C for 5 h at a heating rate of 10 °C min^{-1}. As for the metal catalyst, a commercial SiO_2 (Sigma-Aldrich) was firstly pretreated in an oven at 800 °C for 5 h (10 °C min^{-1}). An aqueous solution of $H_2PtCl_6{\cdot}6H_2O$ (Sigma-Aldrich) at a suitable concentration to obtain 1 wt% Pt content was used for catalyst preparation by incipient wetness impregnation. After that, the catalyst was dried overnight at 100 °C and calcined at 500 °C for 4 h (10 °C min^{-1}) under synthetic air flow (50 mL min^{-1}).

X-ray diffraction (XRD) was performed on a Rigaku Miniflex diffractometer with CuKα radiation (1.540 Å). The diffractograms were obtained in the 2θ range from 10° to 90° with steps of 0.05° s^{-1}.

The porosity of the samples was determined by collecting N_2 adsorption and desorption isotherms at −196 °C using a Micromeritics ASAP 2020 equipment. The estimation of the specific areas was performed using B.E.T. formalism.

The chemical composition of the catalysts was analyzed by X-ray fluorescence spectrometry (XRF) using a S8 Tiger Bruker equipment.

The metal dispersion of the Pt/SiO_2 catalyst was determined using Scanning Transmission Electronic Microscopy (STEM). The examination was performed in a Jeol JEM-2100F microscope operating at 200 kV. The powder sample was firstly ultrasonically dispersed in 2-propanol and then deposited on a carbon-coated copper grid for STEM examination. Dispersion (D) was estimated from the average particle diameter calculated from images collected at different regions of the sample using the expression $d_m = \sum n_i x d_i^3 / n_i x d_i^2$, where n_i is the number of particles with diameters within a specific interval. All measurements were made using the software Axio Vision 4.7.

Thermogravimetric analysis (TG-MS) was carried out on a TA Instruments SDT Q600 coupled to a Dymaxion Ametek mass spectrometer. Samples were heated from 40 °C to 700 °C at a heating rate of 20 °C min^{-1}. Fragment ions at m/z = 18 (H_2O), 44 (CO_2), 48 (SO) and 64 (SO_2) were monitored throughout the analysis.

The infrared spectrum of the ZrO_2–SO_4 solid was collected in a Magna 560 Nicolet spectrometer with 32 scans and a resolution of 4 cm^{-1}. This sample was analyzed in a KBr wafer at 3 wt%.

The acid properties of sulfated zirconia were also determined by infrared spectroscopy using pyridine as a probe molecule. Catalyst self-supported wafer was treated *in situ* in a homemade glass cell at 500 °C for 1 h under high vacuum. Pulses of a 20% O_2–He mixture were applied to the sample, followed by high vacuum for 30 min. The adsorption was carried out by admission of 2 torr of pyridine in the cell at room temperature. Pyridine thermal desorption was monitored over a wide range of temperatures under high vacuum. Spectra were all collected at room temperature with 256 scans and a resolution of 4 cm^{-1}. Absorption bands related to Lewis (1450 cm^{-1}) and Brönsted (1540 cm^{-1}) acid sites were integrated to determine their concentration;[23] the density of the wafer (diameter of 13 mm) and the molar extinction coefficients reported by Datka *et al.*[24] were used for calculations.

The reactions were performed in a three-phase batch Parr-type reactor (300 mL) equipped with mechanical stirrer, automated heating and pressure control. The Pt/SiO_2 catalyst was previously reduced at a H_2 flow of 50 mL min^{-1} at 500 °C for 1 h, with a heating rate of 10 °C min^{-1}. After this procedure, the metal catalyst was mixed with sulfated zirconia in the reactor at different proportions. All runs were carried out using 6.66 mol of xylose and a constant agitation of 600 rpm. Hydrogen was admitted into the reactor and the total pressure was kept constant at 30 bar during the whole experiment. Different temperatures within 110 °C and 170 °C and SO_4/Pt surface molar ratios ranging from 0 to 16 were evaluated. H_2O–2-propanol mixtures were used as solvents in different proportions.

The overall conversion, selectivity and yield of the products were calculated on a molar basis using the equations:

$$\text{Conversion of xylose } (X_{xil}) = \frac{[\text{xylose}]_i - [\text{xylose}]_f}{[\text{xylose}]_i} \times 100$$

$$\text{Selectivity } (S) = \frac{[\text{product}]}{[\text{xylose}]_i - [\text{xylose}]_f} \times 100$$

$$\text{Yield}(Y) = \frac{[\text{product}]}{[\text{xylose}]_i} \times 100$$

All reactions were monitored for a total period of 6 hours and samples were collected at regular intervals. They were analyzed by high performance liquid chromatography (HPLC) on a Waters Alliance e2695 equipment coupled to a photodiode array detector (PDA) and a refractive index detector (RID). The analyses were performed in isocratic elution mode using an aqueous solution of H_2SO_4 at 5 mM as the mobile phase with a flow of 0.7 mL min^{-1}. A Biorad Aminex HPX-87H ion exchange column was used to separate all products. The temperatures of the column and RID were maintained at 65 °C and 50 °C, respectively.

The recyclability of the dual catalyst system was assessed by carrying out three consecutive reaction cycles of 6 hours each. After every run, the liquid medium was drained from the reactor and a new xylose (6.66 mol) solution in a H_2O–2-propanol mixture (1 : 3) was charged in. The reactor was firstly purged with N_2 and then pressurized with H_2 (total pressure of 30 bar); all runs were carried out at 130 °C.

Results and discussion

Both catalysts used in this work were characterized with respect to their most fundamental properties for xylose transformation, particularly the crystalline structure, porosity, bulk chemical composition and surface acidity. A detailed discussion of such properties is provided in the ESI.†

X-ray diffraction patterns indicated that the commercial sulfated zirconia is a crystalline material with tetragonal structure and the Pt/SiO_2 catalyst is an amorphous material due to the commercial silica used as a support (see Fig. S1†). The catalysts presented high surface area and narrow mesopores with mean diameters between 5 and 7 nm and low metal dispersion (see Table S1†). The sulfate complexes are coordinated to ZrO_2 as thermally stable bidentate species (see Fig. S2 and S3†). The acid catalyst presented relatively strong Lewis (101 μmol g^{-1}) and Brönsted (216 μmol g^{-1}) acid sites (see Fig. S4†) as typically described for such solids.[25,26]

Liquid-phase xylose processing under hydrogen pressure was carried out to evaluate the catalyst behavior. Such a reaction is rather complex since a multitude of compounds can be formed, from sugar alcohol and shorter polyols to furanic compounds. A few examples of these products are displayed in Scheme 1.

Xylose can be converted into its ketopentose isomer, xylulose, over Lewis acid sites.[27] The hydrogenation of either monosaccharide over metal centers leads to the formation of xylitol, which may be transformed to shorter polyols if overhydrogenated. Furfural can be produced by dehydration of both xylose and xylulose on Brönsted acid sites. The subsequent hydrogenation of the carbonyl group in furfural results in the production of furfuryl alcohol, the aimed product in this contribution. However, the saturation of C=C bonds on the furan ring yields tetrahydrofurfuryl alcohol. Finally, furan may be produced from furfural decarbonylation, leading to tetrahydrofuran by further hydrogenation.[28]

Firstly, some 1 hour control experiments were performed to allow the comparison of xylose transformation in the homogeneous phase (blank run without any solid catalyst), on the metal catalyst (Pt/SiO_2) and its bare support (SiO_2), on the acid solid catalyst (ZrO_2–SO_4), on the mix of the support and the acid solid catalyst (SiO_2 + ZrO_2–SO_4) and also in the presence of a dual catalyst system composed of the metal and acid solid catalysts (ZrO_2–SO_4 + Pt/SiO_2). The latter run was conducted at an acid/metal site surface molar ratio (SO_4/Pt) of 16. For all these initial tests a binary mixture of H_2O–2-propanol (1 : 1) was used as a solvent and the reactions were conducted at 170 °C. The curves of xylose conversion as a function of reaction time are presented in Fig. 1.

It is clear that in all cases xylose conversion is accomplished, reaching approximately 30% even in the absence of a

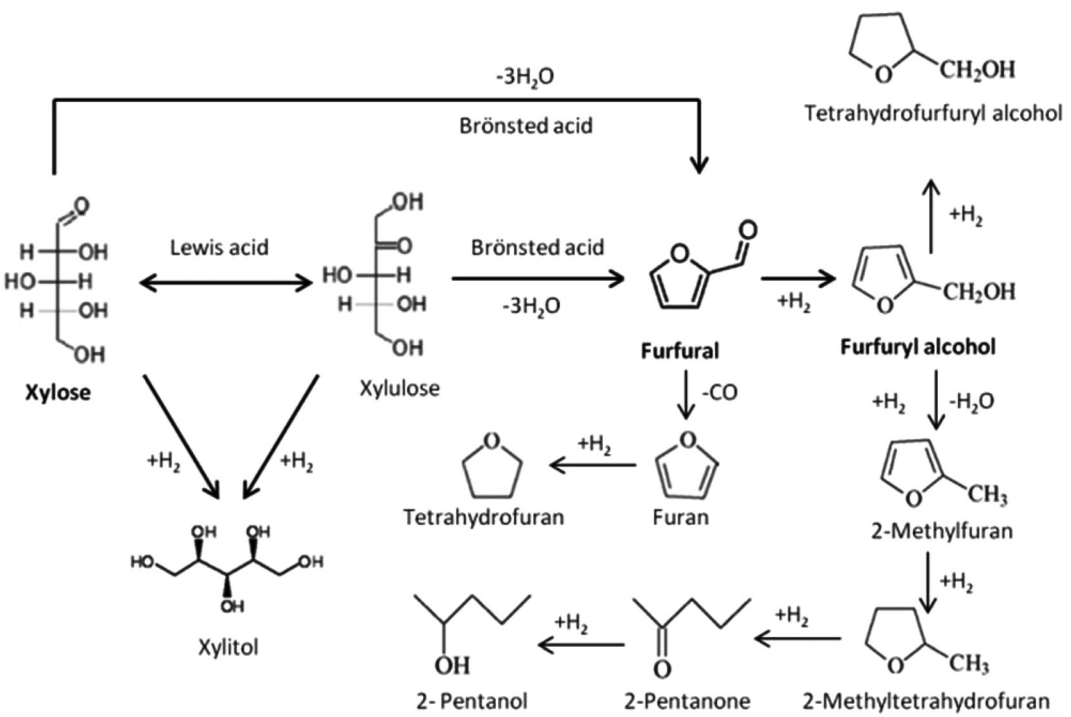

Scheme 1 Reaction scheme with some possible products derived from xylose.

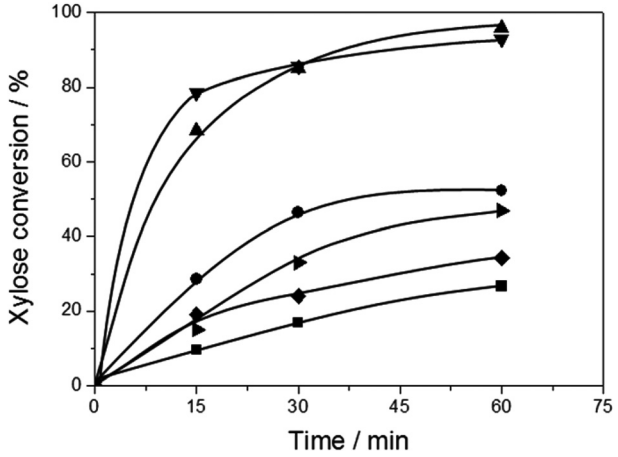

Fig. 1 Xylose conversion for reactions without a catalyst (■), on SiO_2 (▶), Pt/SiO_2 (●), $ZrO_2–SO_4$ (◆), $ZrO_2–SO_4 + SiO_2$ (▼) and over a dual catalyst system ($ZrO_2–SO_4 + Pt/SiO_2$; SO_4/Pt molar ratio = 16) (▲) at T = 170 °C and with H_2O–2-propanol 1 : 1 as a solvent.

catalyst, indicating that some reaction takes place in the homogeneous phase at this temperature. The presence of a catalyst increases the conversion with a notable difference in global activity from the bare support, the solo metal catalyst and the solo acid solid catalyst to the physical mixture of SiO_2 and the acid catalyst or the dual catalyst system with both acid and metal catalysts. Indeed xylose is almost entirely consumed (~96%) after only 1 hour reaction over the dual catalytic systems (physical mixtures), indicating the contribution of the acid catalyst sites to sugar transformation.

Besides the remarkable differences in global activity as expressed by xylose conversion (Fig. 1), the distribution of the products formed also proved to be quite distinct. The yields of the main identified products obtained after a 1 h reaction are summarized in Table 1.

Thermal homogeneous reaction (Table 1, entry 1) promotes essentially the isomerization of xylose to xylulose and the sugar dehydration to furfural. As for SiO_2 and Pt/SiO_2, a marked formation of xylulose as the major product is observed (Table 1, entries 2 and 3), revealing the active role of SiO_2 in the isomerization of xylose to its ketopentose. The $ZrO_2–SO_4$ acid catalyst presents a product distribution closer to that observed for the thermal homogeneous reaction, outlining the low formation of xylulose (Table 1, entry 4). As for $SiO_2 + ZrO_2–SO_4$ (Table 1, entry 5), furfural yield increases considerably, corroborating the previous suggestion concerning the role of SiO_2 in the isomerization of xylulose, which is known to be more rapidly dehydrated to furfural on the Bronsted acid sites[29] provided by $ZrO_2–SO_4$. The synergism between the two catalysts in the dual system is also clear; a noteworthy increase in the yield of the dehydration product (furfural) and the formation of furfuryl alcohol (Table 1, entry 6) can be accomplished. The yield of furfuryl alcohol, however, is pretty low, reaching only 12%. This may be attributed to the occurrence of side reactions under acidic medium (provided by $ZrO_2–SO_4$) under such operating conditions, especially polymerization and condensation, which led to the formation of unidentified high molecular weight products and humins. Indeed, several authors have reported the formation of such compounds during liquid-phase processing of carbohydrates.[6,7,12–14,29]

Table 1 Xylose conversion (X) and yield to xylitol ($Y_{xylitol}$), xylulose ($Y_{xylulose}$), furfural (Y_{FF}) and furfuryl alcohol (Y_{FFA}) at 170 °C and H_2O–2-propanol = 1 : 1 after 1 h reaction

Entry	Sample	X (%)	$Y_{xylitol}$ (%)	$Y_{xylulose}$ (%)	Y_{FF} (%)	Y_{FFA} (%)
1	No catalyst	27	0	11	5	0
2	SiO_2	47	0	23	3	3
3	Pt/SiO_2	52	0	26	0	1
4	$ZrO_2–SO_4$	34	1	8	6	4
5	$SiO_2 + ZrO_2–SO_4$	93	1	2	22	7
6	$Pt/SiO_2 + ZrO_2–SO_4$	96	2	0	42	12

In order to minimize the contribution of the homogeneous reaction as well as the production of heavy compounds, some catalytic tests were performed at lower temperatures. All other reaction conditions were kept the same as those applied in the initial control experiments. The evolution of xylose catalytic conversion with time of reaction is displayed in Fig. 2 (closed markers) along with the curves obtained for blank runs without the use of catalysts (open markers) at the same temperatures. Selectivities at isoconversion are also summarized in Table 2.

Xylose conversion is no longer observed at temperatures up to 130 °C when no catalyst is present. Sugar consumption only began to be relevant from 150 °C, reaching conversions of about 30% after 6 h of reaction (Fig. 2). On the other hand, as expected, the catalytic reactions behaved completely differently and xylose was converted at temperatures as low as 110 °C, increasing gradually with temperature. Roughly complete conversion is achieved after just 4 hour reaction at 150 °C. These

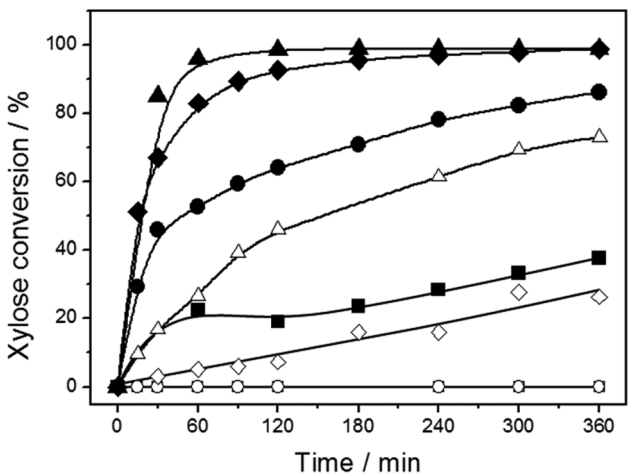

Fig. 2 Conversion of xylose for reactions without a catalyst (open markers) and on the dual catalyst system ($ZrO_2–SO_4 + Pt/SiO_2$; SO_4/Pt molar ratio = 16) (closed markers) with H_2O–2-propanol 1 : 1 as a solvent at different temperatures: 110 °C (■), 130 °C (●), 150 °C (◆) and 170 °C (▲).

Table 2 Xylose conversion (X) and selectivity to xylitol ($S_{xylitol}$), xylulose ($S_{xylulose}$), furfural (S_{FF}) and furfuryl alcohol (S_{FFA})

Entry	SO_3/Pt	T (°C)	H_2O–2-propanol	X[a] (%)	$S_{xylitol}$[b] (%)	$S_{xylulose}$[b] (%)	S_{FF}[b] (%)	S_{FFA}[b] (%)
1	—	110	1 : 1	0	—	—	—	—
2	—	130	1 : 1	0	—	—	—	—
3	—	150	1 : 1	26	2[c]	49[c]	28[c]	19[c]
4	—	170	1 : 1	73	0	40	19	0
5	39	110	1 : 1	38	4[c]	37[c]	8[c]	31[c]
6	39	130	1 : 1	86	2	40	11	15
7	39	150	1 : 1	99	3	20	15	20
8	39	170	1 : 1	99	3	14	38	29
9	13	130	1 : 1	68	5	29	8	16
10	26	130	1 : 1	65	3	15	7	22
11	26	130	1 : 0	54	1	26	7	5
12	26	130	1 : 2	71	2	17	4	33
13	26	130	1 : 3	65	5	20	2	51
14[d]	26	130	1 : 3	55	6	23	2	35
15[e]	26	130	1 : 3	54	6	19	1	29

[a] Conversion after 6 h reaction. [b] Selectivity at isoconversion (~45%). [c] Selectivity at maximum conversion (<45%). [d] Data refer to the second reaction cycle. [e] Data refer to the third reaction cycle.

performances can be attributed solely to the activity of the catalysts.

The distribution of the products was shown to be influenced also by the reaction temperature as disclosed in Fig. 3 and Table 2. Xylulose and furfuryl alcohol are the main products formed at 110 °C, and an interdependence between their production may be roughly envisaged (Fig. 3a).

A minor formation of furfural and xylitol could also be detected. It is conceivable that under these reaction conditions all furfural formed over the solid acid is sequentially hydrogenated on the Pt-based catalyst.

As the temperature increases, the time-resolved profiles of the reaction change considerably. Xylulose formation is no longer detected as the major product and its interdependence with other products gets clearer at 130 °C, a temperature at which xylulose is steadily converted into furfuryl alcohol and furfural upon reaction time (Fig. 3b). It should be outlined that a more balanced formation of furfural and furfuryl alcohol is reached at 130 °C, accomplishing a smooth distribution at 150 °C (Fig. 3c). As a matter of fact, the aldehyde formation was seen to become gradually more significant as temperature increased, the main product being formed at 170 °C (Fig. 3d). This trend is in close agreement with the literature, which reports that xylose dehydration is promoted at such high temperatures.[6,12]

The steady drop in the production of furfuryl alcohol upon reaction temperature should not be disregarded, however. It may be associated with its polymerization to PFA (poly(furfuryl alcohol)), which proceeds by the acid-catalyzed condensation of furfural alcohol units[13] and is reckoned to be thermodynamically favored.[27]

Only negligible formation of xylitol was observed within the whole range of temperatures investigated, which suggests that the hydrogenation of furfural is kinetically favored over xylose reduction to the corresponding sugar alcohol.

The complex dynamics regarding the formation of each product upon temperature can be more sharply disclosed using the temperature-resolved profiles of each detected product as presented in Fig. 4. It seems clear that xylulose plays only an intermediate role in the catalytic transformation of xylose to furanic compounds.

Taking into account these results, further investigation of furfuryl alcohol was carried out at 130 °C, aiming at optimizing the alcohol yields by suppressing its polymerization and other side reactions.

As discussed hereinbefore, the production of furfuryl alcohol takes place as the subsequent reaction of xylose/xylulose dehydration to furfural, each of these reactions proceeding over different components of the dual catalyst system. Therefore it is conceivable that the adjustment of acid and metal sites may tune product distribution. Fig. 5 shows the evolution of the main product selectivity as a function of xylose conversion.

Xylulose presents nearly the same behavior as discussed previously, revealing that xylose isomerization is the first step in sugar conversion. Furfuryl alcohol is always the main product and only a slight difference in its production can be noticed, depending on the SO_4/Pt molar ratio, with selectivity varying within 15–25%. Consistently, the formation of furfural is more meaningfully affected, rising with the concentration of acid sites in the reactor, the ones responsible for promoting dehydration. Finally, xylitol selectivity is permanently low and is even more negligible at higher SO_4/Pt surface molar ratios. It is likely ascribed to the preferential xylose/xylulose consumption to furfural over acid sites due to their higher density in the reaction medium as well as the kinetically favored hydrogenation of the aldehyde as previously observed.

Examination of the solvent effects on catalytic reactions has been carried out over the last few decades for a multitude of organic reactions, especially hydrogenation. By mining the literature, it can be seen that the role of the solvent on catalytic activity and selectivity is rather complex. It may usually be rationalized by hydrogen solubility and solvent polarity[30,31] or even by intermolecular interactions, which requires the

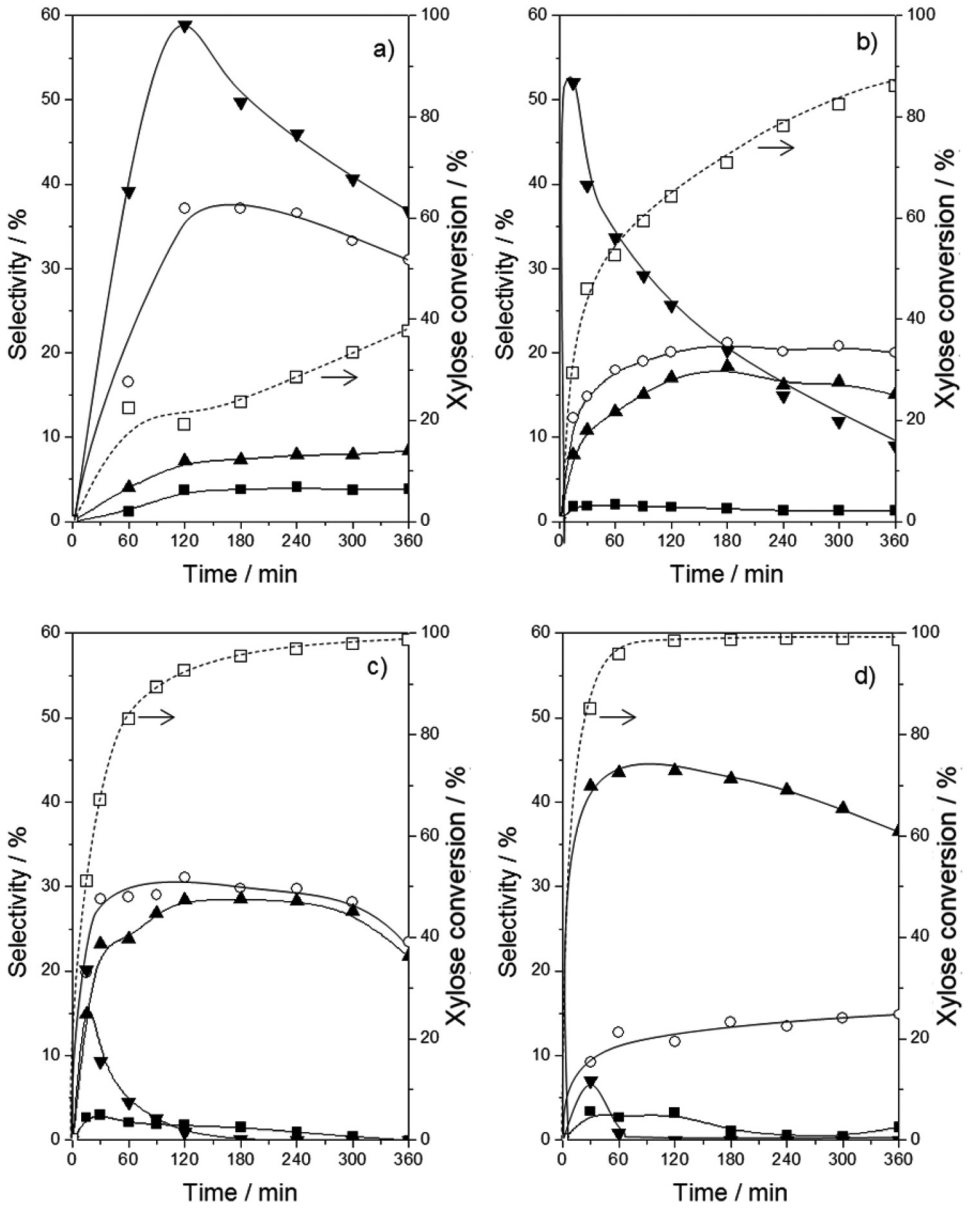

Fig. 3 Xylose conversion (□) and selectivity to xylitol (■), xylulose (▼), furfural (▲) and furfuryl alcohol (○) with H_2O–2-propanol 1 : 1 as a solvent, SO_4/Pt molar ratio = 16 at different temperatures: 110 °C (a), 130 °C (b), 150 °C (c) and 170 °C (d).

knowledge of the liquid structure and dynamics.[32] Concerning specifically the hydrogenation of saccharides, alcoholic solvents have shown an outstanding effect on kinetics, which is ascribed to hydrogen solubility.[30]

In addition to hydrogenation, the solvent effect has also been addressed in studies on carbohydrate dehydration. Furfural production from dehydration of xylose is one of the most studied reactions for which the performances in aqueous, non-aqueous or organic-aqueous biphasic systems have been reported. Toluene,[6,10,11,14,19] DMSO[7–9] and 1-butanol[12,32] are amongst the most investigated solvents. The use of biphasic media has been shown to be quite a successful approach since the produced furfural is transferred to the organic solvent, avoiding its condensation/degradation in the acidic aqueous phase.

In this contribution, any influence caused by the nature of the solvent was investigated at 130 °C with a dual catalyst system with surface molar ratio SO_4/Pt = 8. Aqueous-alcohol monophasic systems were exclusively targeted since there would be no need of extracting furfural (the intermediate product) once it is planned to be hydrogenated immediately afterwards. This investigation was therefore performed by adding increasing amounts of 2-propanol. Lower miscible alcohols (ethanol and methanol) were not exploited, however. Ethanol has been reported to react with furfuryl alcohol, leading to the formation of ethyl levulinate,[28] while sustainable, health issues discouraged the use of methanol.

Binary mixtures of water–2-propanol at 1 : 0, 1 : 1, 1 : 2 and 1 : 3 were used as solvents. It is worth mentioning that no

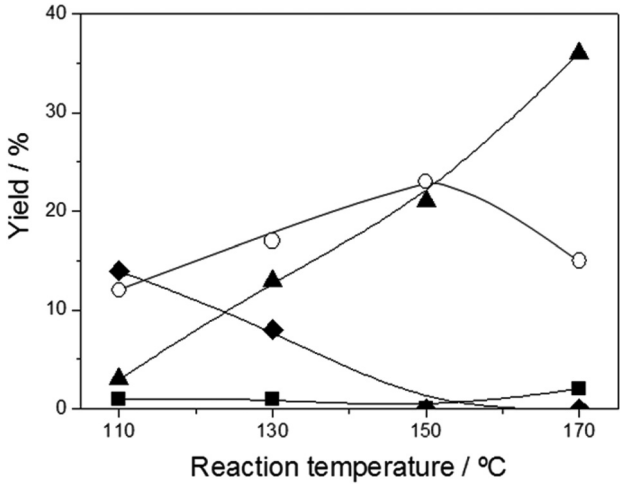

Fig. 4 Yield for xylitol (■), xylulose (◆), FF (▲) and FFA (○) as a function of reaction temperature.

products derived from the acid-catalyzed reaction between 2-propanol and furfuryl alcohol (etherification/dehydration) were formed in any appreciable amount that could allow their detection and identification. Irrespective of the solvent composition, xylose isomerization to xylulose was always observed with maximum selectivity ranging from 40 to 50% and the selectivity drops gradually as the reaction proceeds. Hydrogenation to xylitol also occurred but, as previously seen, the formation of this sugar alcohol was pretty timid reaching selectivities usually below 5%. The patterns found for furfural and furfuryl alcohol, on the other hand, showed that the formation of those chemicals is sensitive to the binary solvent as displayed in Fig. 6.

The curves of selectivity as a function of xylose conversion show that the higher the amount of 2-propanol in the mixture, the higher the selectivity towards furfuryl alcohol and the lower the selectivity towards furfural. Indeed, a selectivity as high as 50% could be achieved for a H_2O–2-propanol ratio of 1 : 3. This is a noteworthy result for the unprecedently reported one-pot production of furfuryl alcohol from xylose. As very recently reported by Kim *et al.*[33] such a performance may be associated with the reduction of the polymerization reaction rate of furfuryl alcohol by the competitive interaction between furfuryl alcohol carbocation and another furfuryl alcohol molecule (decisive for polymerization) and the interaction between the carbocation and the solvent molecules (2-propanol) through hydrogen bonding. Furthermore steric hindrance provided by the alcohol solvent molecules is also claimed to play a role in preventing polymerization.[27–29,34]

Despite the intermolecular interactions and shielding effects, attention should once again be drawn to the substantial decrease in selectivity to furfuryl alcohol when a high conversion is accomplished (Fig. 6). It is possibly a consequence of the formation of condensed products since polymerization is the prevailing reaction at high furfuryl alcohol concentrations due to its reaction kinetics as reported by Maldonado *et al.*[35]

The recyclability of the dual catalyst system was assessed by carrying out three consecutive reaction cycles and the results are presented in Fig. 7 and Table 2. Xylose conversion was 65% with 51% furfuryl alcohol selectivity in the first run (Table 2, entry 13). Nevertheless, catalytic activity exhibited a drop of around 15% in the subsequent cycle (Table 2, entry 14) but kept its stability in a third run (Table 2, entry 15). Selectivity towards furfuryl alcohol, on the other hand, decreased gradually after each catalytic run, reaching 29% in the third

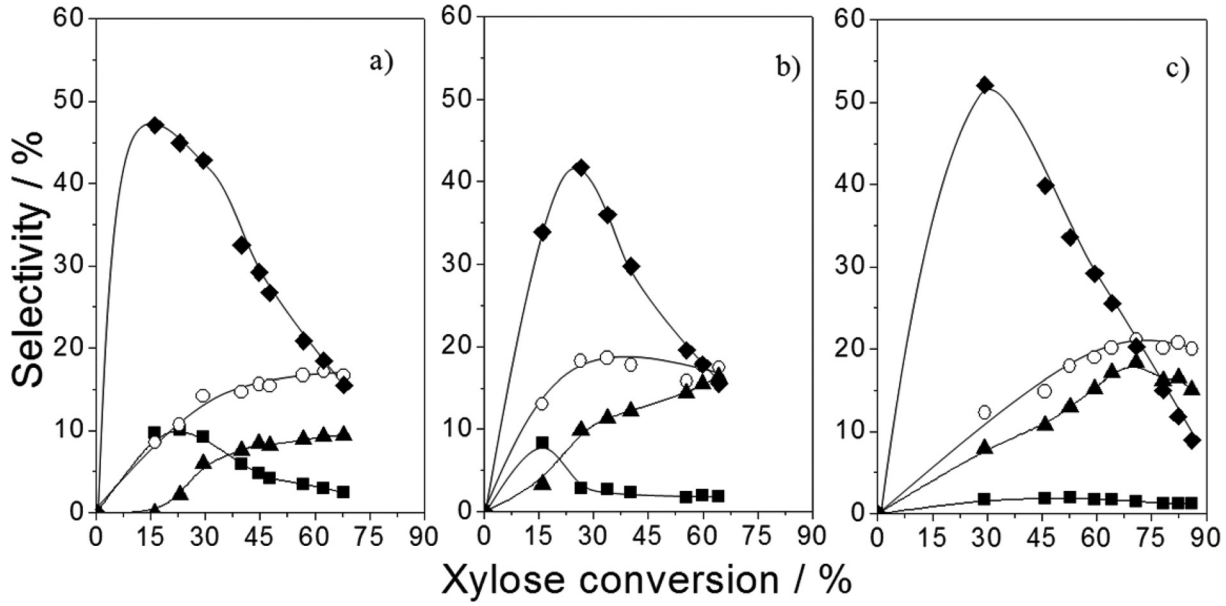

Fig. 5 Selectivity to xylitol (■), xylulose (◆), furfural (▲) and furfuryl alcohol (○) as a function of xylose conversion at T = 130 °C and using H_2O–2-propanol 1 : 1 as a solvent for SO_4/Pt surface molar ratio = 4 (a), 8 (b) and 16 (c).

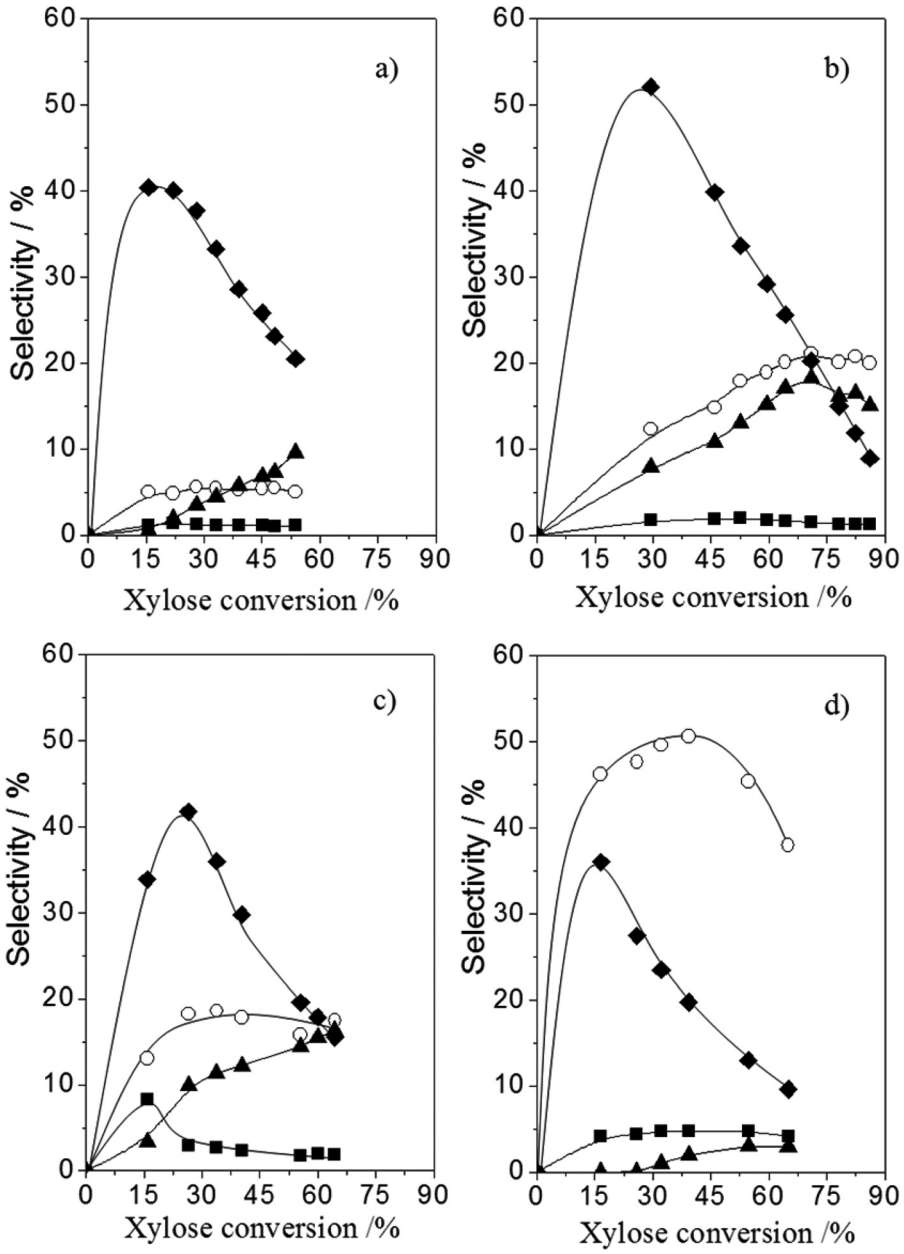

Fig. 6 Selectivity to xylitol (■), xylulose (◆), furfural (▲), and FFA (○) as a function of xylose conversion at T = 130 °C and SO_4/Pt molar ratio = 8 using H_2O–2-propanol as a solvent in the ratios 1 : 0 (a), 1 : 1 (b), 1 : 2 (c) and 1 : 3 (d).

last cycle. Considering that the formation of other products is not affected, which mostly depend on the surface sites in the metal catalyst (either SiO_2 or Pt metal sites), this trend might suggest that the acid solid catalyst in the dual system is undergoing some deactivation.

The original results presented herein showed that it is possible to produce furfuryl alcohol straight from xylose over a heterogeneous dual catalyst system. By tuning the reaction conditions and the balance between acid and metal centers in the catalyst system, both mandatory sites for this one-pot transformation, selectivity and yield can be optimized. The catalytic understanding of this reaction may contribute to the development of other innovative processes based on hemicellulose-derived saccharides, widening the range of green routes to industrial chemicals.

Conclusions

The feasibility of producing furfuryl alcohol from xylose in a one-step process over heterogeneous catalysts was shown. The occurrence of both acid and metal sites was shown to be compulsory to promote the dehydration of xylose to furfural and its further hydrogenation to furfuryl alcohol. The selectivity towards furfuryl alcohol was found to be strongly dependent on the solvent, which can inhibit its polymerization to some extent.

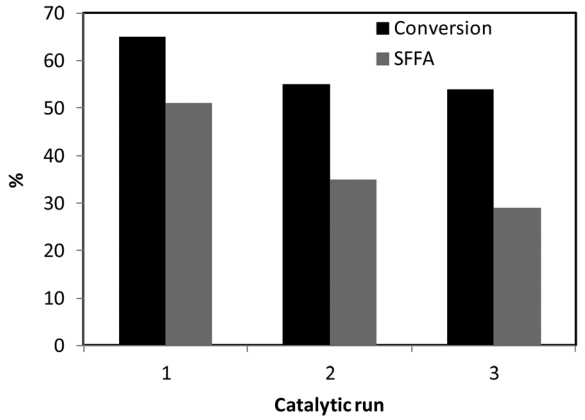

Fig. 7 Conversion of xylose and selectivity to furfuryl alcohol (SFFA) on the dual catalyst system (ZrO_2–SO_4 + Pt/SiO_2; SO_4/Pt molar ratio = 8) at 130 °C and using H_2O–2-propanol 1 : 3 as a solvent after three consecutive runs.

Acknowledgements

The authors acknowledge the financial support from CNPq and FAPERJ. They also thank Ms Flavia de Almeida Ferreira and Ms Renata dos Santos for their valuable assistance in the characterization of the catalysts. Authors acknowledge Mel Chemicals for kindly supplying a ZrO_2–SO_4 sample and Prof. A. Pinto and Ms Cilene Labre from Centro Brasileiro de Pesquisas Físicas (CBPF) for their helpful assistance in STEM analyses.

References

1 A. Corma, S. Iborra and A. Velty, *Chem. Rev.*, 2007, **107**, 2411–2502.
2 J. Serrano-Ruiz, R. Luque and A. Sepúlveda-Escribano, *Chem. Soc. Rev.*, 2011, **40**, 5266–5281.
3 H. Kobayashi and A. Fukuoka, *Green Chem.*, 2013, **15**, 1740–1763.
4 B. Danon, G. Marcotullio and W. de Jong, *Green Chem.*, 2014, **16**, 39–54.
5 W. de Jong and G. Marcotullio, *Int. J. Chem. React. Eng.*, 2010, **8**, A69.
6 C. Moreau, R. Durand, D. Peyron, J. Duhamet and P. Rivalier, *Ind. Crops Prod.*, 1998, **7**, 95–99.
7 A. Dias, M. Pillinger and A. Valente, *J. Catal.*, 2005, **229**, 414–423.
8 A. Dias, M. Pillinger and A. Valente, *Appl. Catal., A.*, 2005, **285**, 126–131.
9 A. Dias, S. Lima, D. Carriazo, V. Rives, M. Pillinger and A. Valente, *J. Catal.*, 2006, **244**, 230–237.
10 A. Dias, M. Pillinger and A. Valente, *Microporous Mesoporous Mater.*, 2006, **94**, 214–225.
11 A. Dias, M. Pillinger and A. Valente, *Catal. Lett.*, 2007, **114**, 151–160.
12 V. Ordomsky, J. Schouten, J. Schaaf and T. Nijhuis, *Appl. Catal., A.*, 2013, **451**, 6–13.
13 E. Gürbüz, S. Wettstein and J. Dumesic, *ChemSusChem*, 2012, **5**, 383–387.
14 X. Shi, Y. Wu, H. Yi, G. Rui, P. Li, M. Yang and G. Wang, *Energies*, 2011, **4**, 669–684.
15 M. Antunes, S. Lima, A. Fernandes, M. Pillinger, M. Ribeiro and A. Valente, *Appl. Catal., A*, 2012, **417–418**, 243–252.
16 A. Mammal, J. Lee, Y. Kim, I. Hwang, N. Park, Y. Hwang, J. Chang and J. Hwang, *Biofuels, Bioprod. Biorefin.*, 2008, **2**, 438–454.
17 P. L. Dhepe and R. Sahu, *Green Chem.*, 2010, **12**, 2153–2156.
18 I. Agirrezabal-Telleria, J. Requies, M. B. Güemez and P. L. Arias, *Green Chem.*, 2012, **14**, 3132.
19 I. Agirrezabal-Telleria, A. Larreategui, J. Requies, M. Güemez and P. Arias, *Bioresour. Technol.*, 2011, **102**, 7478–7485.
20 J. Kijenski, P. Winiarek, T. Paryjczak, A. Lewicki and A. Mikolajska, *Appl. Catal., A*, 2002, **233**, 171–182.
21 B. Nagajara, A. Padmasri, B. Raju and K. Rao, *J. Mol. Catal. A: Chem.*, 2007, **265**, 90–97.
22 A. Merlo, V. Vetere, J. Ruggera and M. Casella, *Catal. Commun.*, 2009, **10**, 1665–1669.
23 R. M. Ravenelle, J. R. Copeland, W. G. Kim, J. C. Crittenden and C. Sievers, *ACS Catal.*, 2011, **1**, 552–561.
24 J. Datka, A. M. Turek, J. M. Jehng and I. E. Wachs, *J. Catal.*, 1992, **135**, 186–199.
25 F. Ramos, A. M. Duarte de Farias, L. E. P. Borges, J. L. Monteiro, M. A. Fraga, E. Sousa-Aguiar and L. G. Appel, *Catal. Today*, 2005, **101**, 39–44.
26 J. Lavalley, R. Anquetil, J. Czyzniewska and M. Ziolek, *J. Chem. Soc., Faraday Trans.*, 1996, **92**, 1263–1266.
27 V. Choudhary, A. Pinar, S. Sandler, D. Vlachos and R. Wolf, *ACS Catal.*, 2011, **1**, 1724–1728.
28 J. Lange, E. Heide, J. Buijtenen and R. Price, *ChemSusChem*, 2012, **5**, 150–166.
29 R. Weingarten, G. Tompsett, W. Conner Jr. and G. Huber, *J. Catal.*, 2011, **279**, 174–182.
30 J. Mikkola, T. Salmi and R. Sjöholm, *J. Chem. Technol. Biotechnol.*, 2001, **76**, 90–100.
31 N. Bertero, A. Trasarti, C. Apesteguía and A. Marchi, *Appl. Catal., A*, 2011, **394**, 228–238.
32 H. Manyar, D. Weber, H. Daly, J. Thompson, D. Rooney, L. Gladden, E. Stitt, J. Delgado, S. Bernal and C. Hardacre, *J. Catal.*, 2009, **265**, 80–88.
33 T. Kim, R. Assary, H. Kim, C. Marshall, D. Gosztola, L. Curtiss and P. Stair, *Catal. Today*, 2013, **205**, 60–66.
34 J. Chheda, G. Huber and J. Dumesic, *Angew. Chem., Int. Ed.*, 2007, **46**, 7164–7183.
35 G. M. González Maldonado, R. S. Assary, J. Dumesic and L. A. Curtiss, *Energy Environ. Sci.*, 2012, **5**, 6981–6989.

